Article

Design and Performance of an Innovative Four-Bed, Three-Stage Adsorption Cycle

Abul Fazal Mohammad Mizanur Rahman [1],*, Yuki Ueda [1], Atsushi Akisawa [1], Takahiko Miyazaki [2] and Bidyut Baran Saha [3,4]

[1] Graduate School of Bio-Applications and System Engineering (BASE), Tokyo University of Agriculture and Technology, 2-24-16, Naka-cho, Koganei-shi, Tokyo 184-8588, Japan; E-Mails: uedayuki@cc.tuat.ac.jp (Y.U.); akisawa@cc.tuat.ac.jp (A.A.)

[2] Faculty of Engineering Sciences, Kyushu University, 6-1 Kasuga-koen, Kasuga-shi, Fukuoka 816-8580, Japan; E-Mail: miyazaki.takahiko.735@m.kyushu-u.ac.jp

[3] Mechanical Engineering Departments, Faculty of Engineering, Kyushu University, 744 Motooka, Nishi-ku, Fukuoka 819-0395, Japan; E-Mail: saha.baran.bidyut.213@m.kyushu-u.ac.jp

[4] International Institute for Carbon-Neutral Energy Research (WPI-I2CNER), Kyushu University, 744 Motooka, Nishi-ku, Fukuoka 819-0395, Japan

* Author to whom correspondence should be addressed; E-Mail: afmmr_ssdl@yahoo.com; Tel./Fax: +81-042-388-7282.

Abstract: The design of a four-bed three-stage adsorption cycle has been proposed to reduce the volume of the six-bed three-stage adsorption cycle. A simulation model for the proposed innovative cycle was developed to analyse the influence of cycle time on the system performance identifying the specific cooling power (*SCP*) and coefficient of performance (*COP*). A particle swarm optimization (PSO) technique was used to optimize the cycle time enabling us to maximize the *SCP*. PSO results showed that the optimal cycle time was decreased with heat source temperature and *SCP* value was proportional to heat source temperature. It was found that the proposed cycle could be driven by waste heat as low as 40 °C, along with coolant at 30 °C. Comparative study of optimized result indicated that the proposed cycle increased the performance significantly over a whole range of temperatures from 40 to 70 °C and reduced two adsorbent beds, compared to the six-bed three-stage cycle.

Nomenclature

A	heat transfer area (m^2)
C_p	specific heat (J kg^{-1} K^{-1})
D_{so}	surface specific heat (m^2 s^{-1})
E_a	activation energy (J kg^{-1})
$ksap$	overall mass transfer coefficient
L	latent heat of vaporization (J kg^{-1})
$\dot{m}$	mass flow rate (kg s^{-1})
P_s	saturated vapour pressure (Pa)
q	fraction of water content that can be adsorbed by the adsorbent (kg kg^{-1})
q^*	fraction of water content that can be adsorbed by the adsorbent under saturation condition (kg kg^{-1})
Q_{st}	isosteric heat of adsorption (J kg^{-1})
R	gas constant (J kg^{-1} K^{-1})
R_p	average radius of silica gel particles (m)
T	temperature (K)
t	time (s)
U	overall heat transfer coefficient (W m^{-2} K^{-1})
W	mass (kg)
Col	cooling water
Hot	hot water
V	valve

Superscripts

b	adsorption/desorption bed
c	condenser
e	evaporator
ads	adsorption
des	desorption
$cool$	cooling water
hot	hot water
$chil$	chilled water

Subscripts

hex	heat exchanger (Copper and Aluminium)
in	inlet
out	outlet
s	silica gel
tot	total
$cycle$	total cycle
w	water
wv	water vapour

1. Introduction

Utilization of waste heat and renewable energy can lead to significant contributions in the reduction of the consumption of fossil fuels. One of the key technologies that allow the utilization of relatively low-grade heat sources, typically below 100 °C, is adsorption heat pump system. It has been established that adsorption heat pumps can produce cooling power utilizing a heat source consuming temperature as low as 40 ℃, along with a coolant at 30 ℃ if a three-stage regenerative scheme is employed [1]. Low-temperature waste heat is commonly found as part of any process in industry or in renewable heat sources, such as solar thermal energy, even in moderate solar radiation regions around the World. Moreover, in most cases, adsorption systems neither use ozone layer depleting gases such as CFCs/HCFCs, nor fossil fuel and electricity as their driving source. Therefore, it is widely considered that adsorption heat pump systems are environmentally-friendly and have energy-saving potential. Moreover, they can not only serve the needs for air-conditioning, refrigeration and ice making purposes, but also can meet the demand pure water through adsorption desalination processes [2–7].

A basic conventional single-stage adsorption system comprises of two adsorbent beds, one condenser and an evaporator [8,9]. Many researchers have studied advanced single-stage adsorption systems such as two-bed mass recovery, three-bed, three-bed mass recovery, and two-bed heat recovery adsorption cycles to improve the performance of the single-stage adsorption cooling system [10,11]. However, the required driving temperature for advanced single-stage adsorption systems is 80 ℃ or higher.

Saha *et al.* [12] proposed a design of a four-bed two-stage adsorption chiller to reduce the temperature of the heat source. They showed numerically that the chiller can utilize solar/waste heat of temperatures below 70 ℃. Alam *et al.* [13] and Hamamoto *et al.* [14] identified the influence of design parameters and operating conditions on the performance of the chiller proposed by Saha *et al.* [12]. Moreover, the modification of the chiller in terms of operating conditions such as re-heat schemes was investigated by Khan *et al.* [15–17], Alam *et al.* [18] and Farid *et al.* [19]. These investigations identified that it can work with a heat source temperature as low as 45 ℃ [20]. Recently, experimental study on a two-stage adsorption freezing machine driven by a low temperature heat source was done by Wang *et al.* [21]. However, the coefficient of performance (*COP*) of a two-stage adsorption cycle was found to be lower than that of the advanced single-stage chillers [22,23].

To increase the performance while keeping the heat source temperature around 45 ℃, Saha *et al.* [24] proposed a design of advanced three-stage chiller and then investigated the effect of different parameters (e.g., cycle time, heat exchanger flow rate and temperature) on system performance [1]. Khan *et al.* [25] improved system performance by adding a re-heat scheme. It was shown that the *COP* of a three-stage adsorption chiller reaches up to 0.3 at 70 ℃ heat source temperature with a cycle time of 4400 s and longer, the heat source temperature can be reduced to as low as 40 ℃ along with a coolant at 30 °C.

The three-stage chiller has six beds (*i.e.*, a pair of beds in each stage) and these beds occupy a large part of the system. Accordingly, the footprint of the three-stage machine is larger than that of the single- and two-stage adsorption machines for the same cooling capacity. This is the drawback of multi-stage systems, therefore, any reduction of the number of adsorbent beds directly contributes to the reduction of system volume.

In the present study, first a design of a four-beds three-stage adsorption system was proposed, instead of a six-beds three-stage adsorption system. Second, cycle time was optimized to maximize the performance of the proposed and former six-bed system to identify the best performance. The particle swarm optimization method was used to obtain the maximum cooling output under standard working conditions. Finally, the performance of the proposed cycle was compared with the optimal performance of former six-bed three-stage adsorption systems.

2. Description of Three-Stage Adsorption Cycle

Advance single-stage adsorption system is used to achieve better performance, and two- and three-stage cycles were proposed to utilize lower heat source temperature. A single-stage adsorption cycle is not operational when the heat source temperature is below 60 ℃ along with a coolant of temperature 30 ℃ or higher. For practical utilization of these temperatures in adsorption system operation, higher staged regeneration is necessary. In this regard, Saha *et al.* [26] first proposed a six-bed three-stage adsorption cycle. The schematic diagram of the system is shown in Figure 1a and its operation mode is given in Table 1a. In this case, three pairs of adsorber/desorber heat exchanger beds *i.e.*, Bed 1-Bed 2, Bed 3-Bed 4, and Bed 5-Bed 6 were used in the lower cycle, intermediate cycle and upper cycle, respectively. In the proposed four-bed three-stage cycle, in order to reduce the physical geometry of the system, four adsorption/desorption beds in the intermediate and upper cycles were replace by two adsorption/desorption beds. To make the adsorption cycle competitive in the market, it is necessary to consider economical issues as well as the total size of system. A schematic of the proposed cycle with modifications (indicated by arrow marks) is shown in Figure 1b. In the proposed case Bed 3 and Bed 4 can work instead of Bed 3-Bed 4 and Bed 5-Bed 6 in the former cycle, respectively, whereas Bed 1 and Bed 2 were kept as in the former system. The operation mode of the proposed system is given in Table 1b. Operation strategy has taken into account the relatively longer adsorption time compared to the desorption time, whereas in the former cycle adsorption and desorption time were chosen equal. In the first half cycle of the proposed system, Bed 3 adsorbs vapour from Bed 1 and then it transfers to the condenser *via* Bed 4. Similarly, in the second half cycle, it adsorbs vapour from Bed 2 and then transfers in to the condenser in similar way. As a result, Bed 3 and Bed 4 are completing two full cycles, while Bed 1 and Bed 2 are completing only one full cycle operation at the same time.

The proposed three-stage adsorption cycle consists of four adsorber/desorber heat exchangers, namely Bed 1, Bed 2, Bed 3 and Bed 4, one evaporator and one condenser (Figure 1b). Silica-gel and water have been chosen as adsorbent-refrigerant pair because the regenerative temperature of silica gel is lower than that of other adsorbents and water has large latent heat of vaporization.

Figure 1. Schemata of (**a**) six-bed, three-stage chiller of Saha *et al.* [1] and (**b**) proposed design of four-bed, three-stage adsorption cycle with operation mode A (see Table 1b).

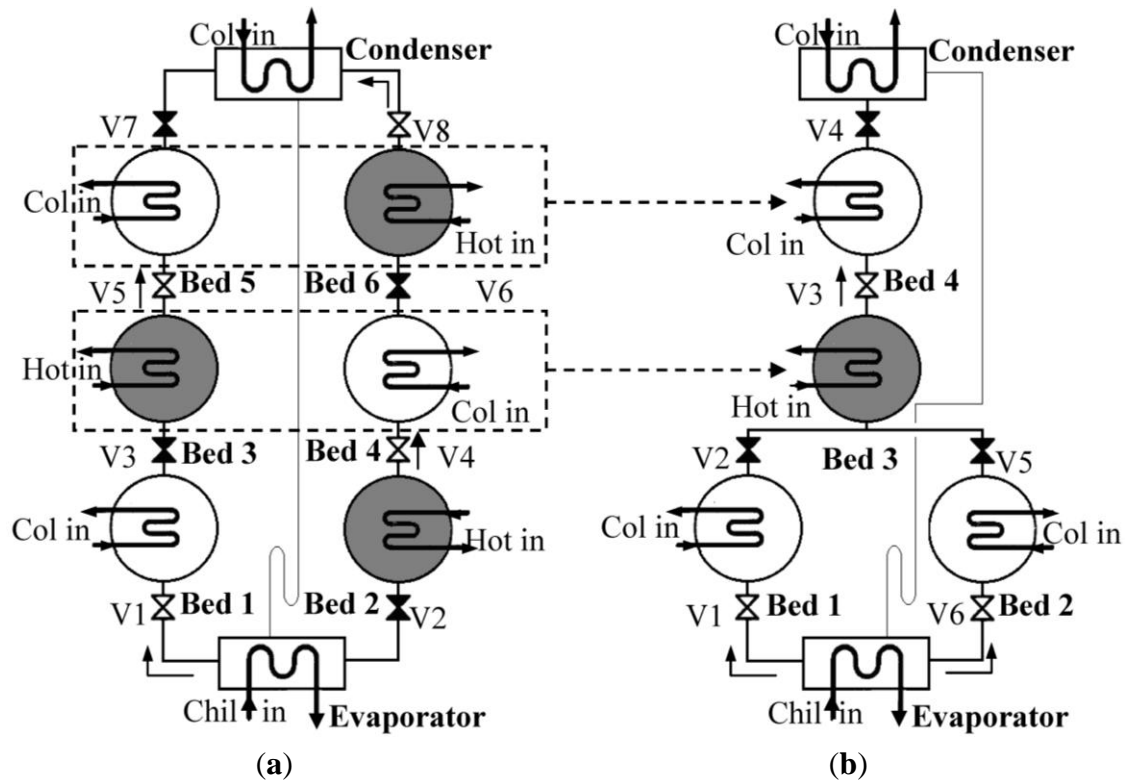(**a**)　　　　　　　　　　　　　　　　　　　　(**b**)

Table 1. Operation mode of former six-bed three-stage cycle and proposed four-bed three-stage cycle with optimal cycle time (in second) at 50 ℃ heat source temperature.

(a) Former six-bed three-stage cycle

| Mode	A	B	C	D
	τ_1	τ_2	τ_1	τ_2
Bed 1	225.9	8.2	225.9	8.2
Bed 2	225.9	8.2	225.9	8.2
Bed 3	225.9	8.2	225.9	8.2
Bed 4	225.9	8.2	225.9	8.2
Bed 5	225.9	8.2	225.9	8.2
Bed 6	225.9	8.2	225.9	8.2

(b) Proposed four-bed three-stage cycle

Mode	A	B	C	D	E	F	G	H
	τ_1	τ_2	τ_1	τ_2	τ_1	τ_2	τ_1	τ_2
Bed 1	129.9	7.9	129.9	7.9	275.6			
Bed 2			405.5			7.9	129.9	7.9
Bed 3	129.9	7.9	129.9	7.9	129.9	7.9	129.9	7.9
Bed 4	129.9	7.9	129.9	7.9	129.9	7.9	129.9	7.9
Valve On	1, 3, 6	6	2, 4, 6	6	1, 3, 6	1	1, 4, 5,	1
Valve Off	2, 4, 5	1, 2, 3, 4, 5	1, 3, 5	1, 2, 3, 4, 5	2, 4, 5	2, 3, 4, 5, 6	2, 3, 6	2, 3, 4, 5, 6

☐ Desorption　　■ Pre-cooling　　■ Adsorption　　■ Pre-heating

The main advantage of the three-stage cycle is the possible utilization of lower grade heat sources than possible with single-stage and two-stage adsorption cycles. For example, a temperature of 50 ℃ is enough to drive the three-stage cycle. However, such low temperature is not enough to pressurize the vapour from the evaporator up to the condenser pressure in a single stage system. The vapour needs to be pressurized three times in the cycle through three-stage adsorption-desorption processes. The first stage pulls up the vapour from evaporator pressure to a certain pressure level, the second stage pulls up an intermediate pressure and then the third stage pushes up the vapour from the intermediate pressure to the condenser pressure.

The Bed 1 and Bed 2 are working at low temperature and pressure (close to the evaporator pressure), Bed 3 is working at intermediate temperature and pressure and Bed 4 is working at higher temperature and pressure (close to the condenser pressure). The conceptual Dühring diagram is shown in Figure 2. The cyclic diagrams a-b-c-d-a, e-f-g-h-e and i-j-k-l-i indicate the lower, intermediate and upper cycle, respectively. All beds are completing four thermodynamic stages, *i.e.*, pre-heating, desorption, pre-cooling and adsorption stage, which are accordingly followed by the sides a-b, b-c, c-d and d-a, and e-f, f-g, g-h and h-e for the lower and intermediate cycle, respectively. Similarly, the sides i-j, j-k, k-l and l-i indicate the modes pre-heating, desorption, pre-cooling and adsorption stage of Bed 4, respectively.

Figure 2. Conceptual Dühring diagram of the proposed cycle.
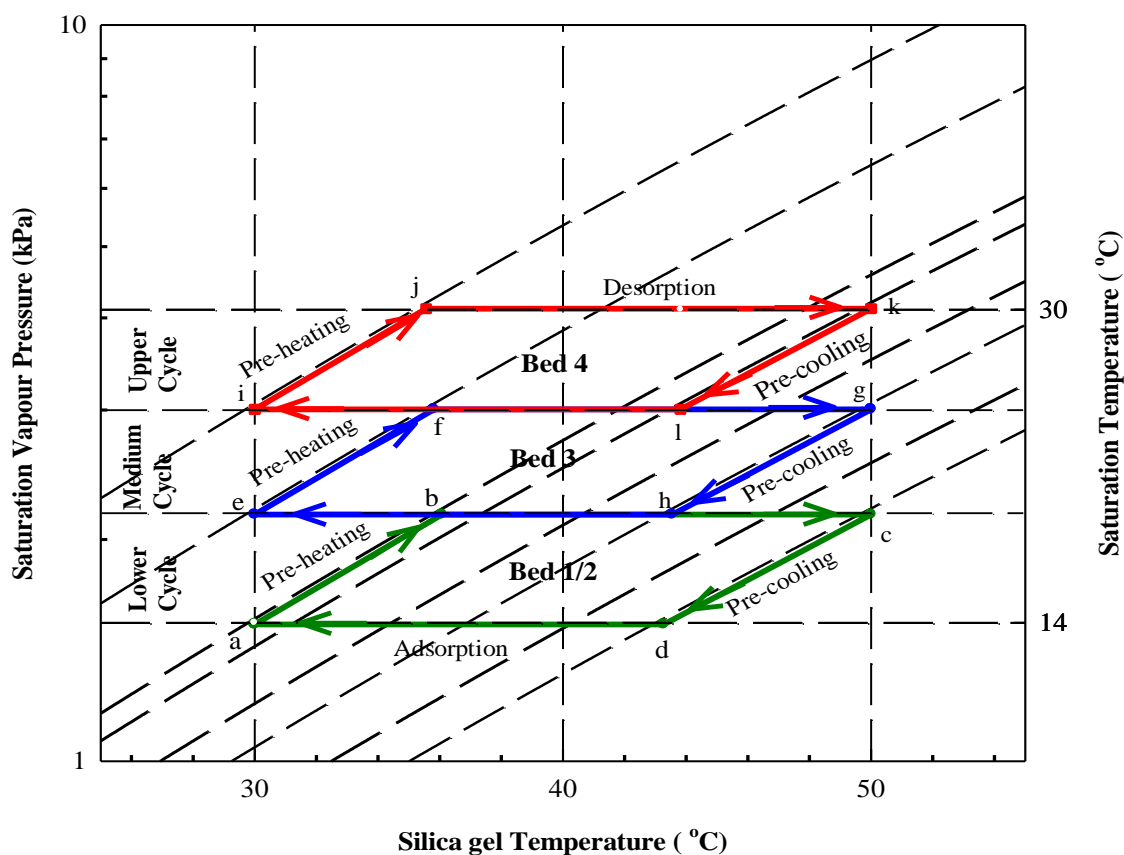
To complete full cycle operation, each bed is to complete eight operational modes, namely A, B, C, D, E, F, G and H, as shown in Table 1b, whereas the former cycle needed four operation modes. The number of operation mode was increased to choose a longer adsorption time compared to desorption time. In Mode A, Bed 1 and Bed 2 are in a cooling state when cooling water is passed through both beds and are connected with the evaporator to adsorb refrigerant vapour from it. This process is called adsorption mode. At the same time the evaporator's lower temperature and pressure is maintained so that water could easily vaporize by seizing heat from chilled water. Bed 2 remains in the adsorption stage up to end of mode E. On the other hand Bed 3 and Bed 4 are connected each other and Bed 3 is heated with hot water to released it own refrigerant vapour to Bed 4. At the same time Bed 4 is cooled with cooling water passing through it to release the adsorption heat.

In mode B, Bed 1 is disconnected from the evaporator and the other two beds (*i.e.*, Bed 3 and Bed 4) are disconnected each other by closing the connecting valve "V3". Then Bed 1 and Bed 4 are heated by hot water to increase their pressure, which is called pre-heating mode and Bed 3 is cooled down by cooling water to reduce its pressure, which is called pre-cooling mode. When the pressures of Bed 1 and Bed 3 become nearly equal, then both are connected each other by opening the connecting valve (*i.e.*, V2), which is starting point of mode C. In this mode, Bed 1 is heated by hot water and Bed 3 is cooled by cooling water, which is called desorption mode for Bed 1 and adsorption mode for Bed 3. Bed 1 is desorbing its adsorbed vapour to the Bed 3, and Bed 3 is adsorbing vapour from Bed 1 during this mode. On the other hand when the pressure of Bed 4 becomes equal to the condenser pressure then it connected with the condenser by opening the connecting valve (V4) to release its own refrigerant vapour to condenser and it is called the desorption of Bed 4 (*i.e.*, mode C). In this mode, adsorbed refrigerant is removed from the bed and goes to the condenser. Then refrigerant vapour is condensed inside condenser and condensation heat is removed by cooling water. Finally, condensed refrigerant goes to the evaporator via a U shape tube.

Mode D is called pre-cooling for Bed 1 and Bed 4, and pre-heating mode for Bed 3, while beds are isolated from other parts of the cycle. In this case Bed 1 is cooled by cooling water to reduce its pressure to the evaporator pressure and then it is connected with the evaporator by opening the connecting valve (V1), which is called adsorption process and starting point for mode E. This process will continue to the end of mode H. Meanwhile, Bed 3 is heated by hot water to increase its pressure and Bed 4 is cooled with cooling water passing through it. When the pressure of both beds becomes equal then both are connected with each other by opening connecting valve V3. This is the starting point of Mode E, which is similar to mode A. Through these modes the first half cycle (from mode A to D) of Bed 3 and Bed 4 are completed and the second half cycle (from mode E to H) is started. The mechanism of modes E, F, G and H of Bed 3 is similar to the modes A, B, C and D, but during these modes, Bed 3 is connected with Bed 2 instead of Bed 1 (*i.e.*, mode G) and vapour is transferred among Bed 2 and Bed 3. In the second half cycle Bed 4 acts exactly the same as in the first half cycle.

3. Simulation Methods and Materials

In the analysis, it is assumed that the temperature, pressure and refrigerant concentration throughout the adsorbent bed are uniform. For the specific heats of metals, adsorbent and adsorbate inside the heat exchanger and for adsorption heat, average values are adopted throughout the entire temperature range.

Moreover, both adsorption and desorption occur at constant pressure, thus specific heat is chosen as C_p. Refrigerant mass flows between evaporator and adsorber, condenser and desorber, adsorber and desorber are taken as equivalent. Total work of the system is considered as zero and total heat is mainly taken into account. Under the above assumptions, the energy balance of the system is explained in following sections.

3.1. Adsorption and Desorption Energy Balance

The heat transfer equation for the adsorption/desorption bed can be written as:

$$T_{out}^{col/hot} = T^b + (T_{in}^{col/hot} - T^b) \cdot \exp\left(-\frac{(U \cdot A)_{hex}^b}{\dot{m}_w^{col/hot} \cdot C_{p,w}} \right) \tag{1}$$

where heat transfer fluid temperature $T_{in}^{col/hot}$ and $T_{out}^{col/hot}$ denote cooling water temperature upon adsorption and hot water temperature upon desorption. T^b stands for adsorption/desorption bed temperature. Heat transfer is fully depending on heat transfer coefficient U_{hex}^b and heat transfer area A_{hex}^b of bed.

The energy balance equation for the adsorption/desorption bed is given below:

$$W_s^b C_{p,s} \frac{dT^b}{dt} + W_s^b C_{p,w} \frac{d(q^{ads/des} \cdot T^b)}{dt} + (W \cdot C_p)_{hex}^b \frac{dT^b}{dt} = \dot{m}_w^{col/hot} c_{p,w} (T_{in}^{col/hot} - T_{out}^{col/hot}) + W_s^b Q_{st} \frac{dq^{ads/des}}{dt}$$
$$ - \alpha . W_s^b C_{p,wv} (T^b - T^e) \frac{dq^{ads/des}}{dt} \tag{2}$$

The same equation is used for adsorption and desorption purposes. During adsorption both $T_{in}^{col/hot}$ and $T_{out}^{col/hot}$ represent the cooling water temperature and during desorption they represent the hot water temperature. The left-hand side of the equation indicates the amount of sensible heat required to cool or heat the silica-gel (*s*), water (*w*) as well as metallic parts of the heat exchanger (*hex*) during adsorption or desorption. The first term of the right hand side stands for the total amount of heat released to the cooling water upon adsorption or provided by the hot water upon desorption, the second term for the adsorption heat release or desorption heat input and last term for the sensible heat of the adsorbed vapour. α is either 0 or 1 depending on whether the bed is working as a desorber or adsorber. The heat balance equation [Equation (2)] does not consider the external heat losses to the environment.

3.2. Evaporator Energy Balance

The heat transfer equation of evaporator can be expressed as:

$$T_{out}^{chil} = T^e + (T_{in}^{chil} - T^e) \cdot \exp\left(-\frac{(U \cdot A)_{hex}^e}{\dot{m}_w^{chil} \cdot C_{p,w}} \right) \tag{3}$$

where T_{out}^{chil} and T_{in}^{chil} indicate the chilled water inlet and outlet temperature, respectively; T^e is the evaporator temperature; and A_{hex}^e and U_{hex}^e are the heat transfer area and heat transfer coefficient of evaporator, respectively. The energy balance equation of evaporator is given below:

$$[W_w^e(t)C_{p,w} + (W \cdot C_p)_{hex}^e]\frac{dT^e}{dt} = -L_w W_s^b \frac{dq^{ads}}{dt} - W_s^b C_{p,w}(T^c - T^e)\frac{dq^{des}}{dt} + \dot{m}_w^{chil} c_{p,w}(T_{in}^{chil} - T_{out}^{chil}) \tag{4}$$

where $W_w^e(t)$ is the mass of water inside the evaporator that is changing with cycle time due to adsorption and desorption process and L_w is the latent heat of vaporization. The left hand side of the equation indicates the sensible heat required by the liquid refrigerant (water) and the metal of heat exchanger tube of evaporator. The first term of the right hand side represents the latent heat for the adsorbed refrigerant; the second term represents the sensible heat required to cool down the incoming condensed refrigerant from the condensation temperature; and the last term represents the total amount of heat loss by the chilled water.

3.3. Condenser Energy Balance

The heat transfer equation of the condenser can be written as:

$$T_{out}^{c,col} = T^c + (T_{in}^{c,col} - T^c) \cdot \exp\left(-\frac{(U \cdot A)_{hex}^c}{\dot{m}_w^{c,col} \cdot C_{p,w}}\right) \tag{5}$$

where A_{hex}^c and U_{hex}^c is the heat transfer area and heat transfer coefficient of condenser, respectively.

The energy balance equation of the condenser is as follows:

$$[W_w^c C_{p,w} + (W \cdot C_p)_{hex}^c]\frac{dT^c}{dt} = [-L_w - C_{p,wv}(T^{b,des} - T^c)]W_s^b \frac{dq^{des}}{dt} + \dot{m}_w^{c,col} c_{p,w}(T_{in}^{c,col} - T_{out}^{c,col}) \tag{6}$$

The left hand side of the equation represents the sensible heat required by the liquid refrigerant and the metallic parts of heat exchanger tubes due to the temperature variations in the condenser. The first part of the right hand side represents the latent heat of vaporization (L_w) for the desorbed refrigerant; the second term represents the sensible heat due to vapour transfer from desorber to the condenser; and the last term takes into account the total amount of heat released to the cooling water.

3.4. Adsorption and Desorption Rate

The adsorption/desorption rate can be express as [27]:

$$\frac{dq^{ads/des}}{dt} = ksap(q^* - q^{ads/des}) \tag{7}$$

where the overall mass transfer coefficient (*ksap*) for adsorption is given by:

$$ksap = 15 \cdot D_S/(R_p)^2 \tag{8}$$

Here R_p denotes the average radius of a silica gel particle. The adsorption rate is controlled by surface diffusion inside the gel particle and surface diffusivity (D_S), which can be expressed by Arrhenius equation as a function of temperature as:

$$D_S = D_{so} \exp\left(\frac{-E_a}{R \cdot T}\right) \tag{9}$$

where D_{so} is a pre-exponential term whose value is taken as 2.54×10^{-4} m^2 s^{-1} [28]. E_a denotes activation energy; R denotes gas constant and T stands for temperature.

q^* is the adsorption uptake at equilibrium state that can be expressed as [29]:

$$q^* = \frac{0.8 \times [P_s(T_w)/P_s(T_s)]}{1 + 0.5 \times [P_s(T_w)/P_s(T_s)]} \tag{10}$$

where $P_s(T_w)$ and $P_s(T_s)$ are the saturation vapour pressure at temperatures T_W (water vapour) and T_S (silica gel), respectively. Antoine correlates the saturation pressure and temperature, which can be expressed as:

$$P_s = 133.32 \cdot \exp[18.3 - 3820/(T - 46.1)] \tag{11}$$

3.5. Mass Balance

Total mass of refrigerant in the system was assumed constant. The rate of change of the mass of liquid refrigerant can be expressed through the following equation:

$$\frac{dW_w^e}{dt} = -W_s^b \left(\frac{dq^{des-con}}{dt} + \frac{dq^{ads-evp}}{dt} \right) \tag{12}$$

where W_s^b is the mass of silica gel packed in each bed and W_w^e is the mass of liquid refrigerant in the evaporator. Superscripts "*des-con*" and "*ads-evp*" stand for the vapor flow from desorber to condenser and evaporator to adsorber, respectively. In this case, vapour transfer of Bed 3 was not taken into account. It was assumed that it desorbed all refrigerant vapour it adsorbed.

3.6. System Performance

The performance of three-stage adsorption cycle is mainly characterized by specific cooling power (*SCP*), which is the cooling capacity *per* unit mass of adsorbent and coefficient of performance (*COP*), which is the ratio between heat released by the evaporator and heat source input to the bed, these can be calculated by using the following equations:

Specific cooling power (*SCP*):

$$SCP = C_{p,w} \int_0^{t_{cycle}} \dot{m}_w^{chil}(T_{in}^{chil} - T_{out}^{chil})dt / t_{cycle} W_{s,tot} \tag{13}$$

where $\dot{m}_w^{chil}$ is the chilled water flow rate; T_{in}^{chil} and T_{out}^{chil} are indicating the chilled water inlet and outlet temperature; and t_{cycle} and $W_{s,tot}$ are indicating the total cycle time and total mass of silica-gel of the system.

Coefficient of performance (*COP*):

$$COP = \frac{C_{p,w} \int_0^{t_{cycle}} \dot{m}_w^{chil}(T_{in}^{chil} - T_{out}^{chil})dt}{\dot{m}_w^{hot} C_{p,w} \int_0^{t_{cycle}} (T_{in}^{hot} - T_{out}^{hot})dt} \tag{14}$$

where $\dot{m}_w^{hot}$ is indicating the hot water flow rate in the desorption bed; and T_{in}^{hot} and T_{out}^{hot} are indicating hot water inlet and outlet temperature, respectively.

3.7. Optimization Procedure

A complete simulation program was developed using MATLAB (MathWorks, Natick, MA, USA) software to solve the equations mentioned above. Adsorption/desorption rate equation, energy balance equation of beds, condenser and evaporator, and mass balance equation have been solved simultaneously using MATLAB ode45 solver. All input parameters such as adsorbent-refrigerant properties, flow rates of heat transfer fluids and heat exchangers specifications were initially given as those for which the system cyclic operation can be continued.

Particle swarm optimization (PSO) methodology was first introduced in 1995 [30] to optimize the nonlinear function based on a swarm of particles (e.g., birds and fishes). These particles are moved around in the search-space according to formulae. The movements of the particles are guided by their own best known position (*i.e.*, personal best) as well as the entire swarm's best known position (*i.e.*, group best). When better positions are being discovered these will then come to guide the movements of the swarm. The formula to update a particle's velocity and position can be written as:

$$v_i^{t+1} = v_i^t + C_1 \cdot r_1 \cdot (p_i^t - x_i^t) + C_2 \cdot r_2 \cdot (p_g^t - x_i^t) \tag{15}$$

$$x_i^{t+1} = x_i^t + v_i^{t+1} \tag{16}$$

where x_i and v_i are the position and velocity of the *i*th particle. p_i is the personal best position that the *i*th particle had reached and p_g, is the group best position that all the particles had reached. t represents the iteration number. r_1 and r_2 are two random numbers between 0 and 1. C_1 and C_2 are two constant numbers, which are often called the acceleration coefficients. In this study, PSO was applied to optimize the cycle time based on maximum value of *SCP*, whereas *SCP* was chosen as the objective function and cycle time (*i.e.*, τ_1 and τ_2) was chosen as the variable. In PSO, a particle holds the values of variables and updates the values toward the optimal solution. After a number of iterations, all the particles hold the same value and the objective function value is maximized. In this case, the number of particles and the number of iterations were considered as 24 and 1500, respectively. It was observed that all particles reached their best position around 500 iterations.

4. Results and Discussion

The simulation program developed for the proposed four-bed three-stage adsorption cycle was operated by adopting the basic input parameters and standard working conditions as presented in Table 2 [23]. The cycle time, operating time of each mode (*i.e.*, τ_1 and τ_2), is one of the most important parameters of the system and effectively influences the overall performance. The specific cooling power (*SCP*) represents the cooling capacity per unit quantity of adsorbent, and therefore it is a useful index for minimizing the size of the system. At first the cycle time was optimized based on the maximization of *SCP* using the PSO procedure. Cycle time of the system was optimized using various heat source temperatures varying from 40 to 70 °C with an increment of 5 °C by keeping outlet temperature of the chilled water at 9 °C. Accordingly, the chilled water flow rate was optimized

simultaneously with cycle time to adjust the chilled water outlet at a constant temperature. Figure 3 shows that optimum cycle time of the proposed system decreases with the increase of heat source temperature. Total optimal cycle time is the sum of the cycle time of all modes (Table 1). The cycle time ratio is defined as the ratio of τ_1 or τ_2 time of different operation modes to the total cycle time. Figure 4 represents the optimal cycle time ratio of the system for different heat source temperatures. It was observed that the cycle time ratios for τ_1 and τ_2 were slightly decreased and increased with heat source temperature, respectively.

Table 2. Basic input parameters and standard working conditions.

(a) Basic input parameters		
Parameters	**Value**	**Units**
Isosteric heat of adsorption, Q_{st}	2.80×10^6	$J\,kg^{-1}$
Activation energy, E_a	4.2×10^4	$J\,mol^{-1}$
Surface specific heat, D_{so}	2.54×10^{-4}	$m^2\,s^{-1}$
Gas constant, R	8.314	$J\,mol^{-1}\,K^{-1}$
Average radius of silica gel particles, R_p	0.30×10^{-3}	m
Specific heat of water, $C_{p,w}$	4.18×10^3	$J\,kg^{-1}\,K^{-1}$
Specific heat of water vapour, $C_{p,wv}$	1.89×10^3	$J\,kg^{-1}\,K^{-1}$
Latent heat of water vaporization, L_w	2.50×10^6	$J\,kg^{-1}$
Specific heat of copper, $C_{p,Cu}$	386.00	$J\,kg^{-1}\,K^{-1}$
Specific heat of aluminium, $C_{p,Al}$	905.00	$J\,kg^{-1}\,K^{-1}$
Specific heat of silica-gel, C_s	924.00	$J\,kg^{-1}\,K^{-1}$
Heat transfer area of bed, A_{hex}^b	0.61×16	m^2
Heat transfer area of evaporator, A_{hex}^e	6.00	m^2
Heat transfer area of condenser, A_{hex}^c	2.00	m^2
Overall heat transfer coefficient of condenser, U_{hex}^c	3070	$W\,m^{-2}\,K^{-1}$
Overall heat transfer coefficient of desorption bed, U_{hex}^b	4898	$W\,m^{-2}\,K^{-1}$
Overall heat transfer coefficient of adsorption bed, U_{hex}^b	3347	$W\,m^{-2}\,K^{-1}$
Overall heat transfer coefficient of evaporator, U_{hex}^e	1251	$W\,m^{-2}\,K^{-1}$
Mass of silica-gel in bed, W_s^b	16.00	kg
Mass of heat exchanger (Cu) in bed, W_{hex}^b	12.67	kg
Mass of heat exchanger (Al) in bed, W_{hex}^b	16.87	kg
Mass of heat exchanger in evaporator, W_{hex}^e	674.0	kg
Mass of water in evaporator, W_w^e ($t = 0$)	61.0	kg
Mass of water in condenser, W_w^c	24.98	kg
Mass of heat exchanger in condenser, W_{hex}^c	12.8	kg
(b) Standard working conditions		
Hot water inlet temperature in bed, T_{in}^{hot}	40–70	℃
Hot water flow rate in bed, $\dot{m}_w^{hot}$	1.0	$kg\,s^{-1}$
Cooling water inlet temperature in bed, T_{in}^{col}	30	℃
Cooling water flow rate in bed, $\dot{m}_w^{col}$	1.0	$kg\,s^{-1}$
Cooling water inlet temperature in condenser, $T_{in}^{c,col}$	30	℃
Cooling water flow rate in condenser, $\dot{m}_w^{c,col}$	0.8	$kg\,s^{-1}$
Chilled water inlet temperature, T_{in}^{chil}	14	℃
Chilled water outlet temperature, T_{out}^{chil}	9	℃

Figure 3. Optimal cycle time of the proposed cycle for different heat source temperature.
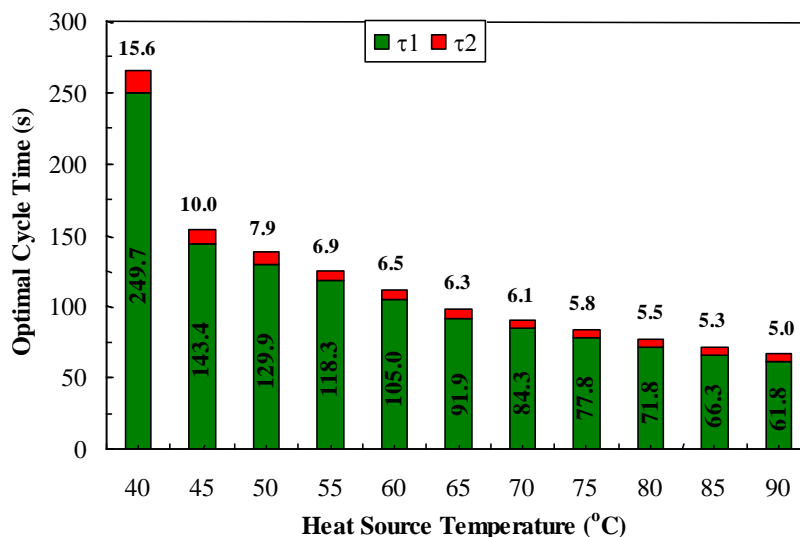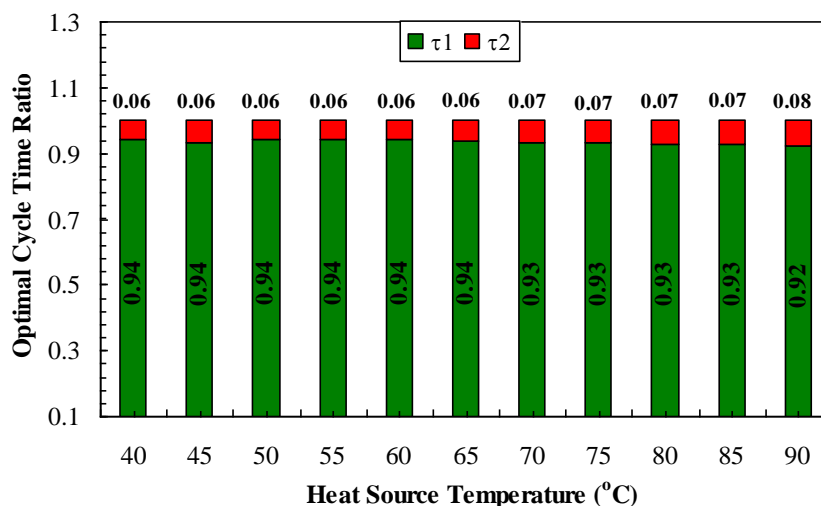

Figure 4. Optimal cycle time ratio of the proposed cycle for different heat source temperature.

Similarly, decreasing optimal cycle time with heat source temperature was also observed for the former six-bed three-stage cycle (Figure 5), but the optimal cycle time ratio of the former cycle indicated an opposite trend, *i.e.*, τ_1 and τ_2 were decreased and increased with heat source temperature, respectively (Figure 6). It is noted that both systems are giving shorter pre-cooling/pre-heating (*i.e.*, τ_2) times.

The variation of chilled water flow rate with heat source temperature for both cycles is shown in Figure 7. It was observed that average chilled water flow rate increases with the increase of driving heat source temperature. Since, heat removal from the chilled water increased with heat source temperature and to keep a constant average chilled water outlet temperature of 9 °C, chilled water flow rate was increased. It was observed that the chilled water flow rate was similar for both cycles, This is due to both systems having two beds (*i.e.*, Bed 1 and Bed 2) in the bottom cycle with equal masses of silica gel and producing similar effects.

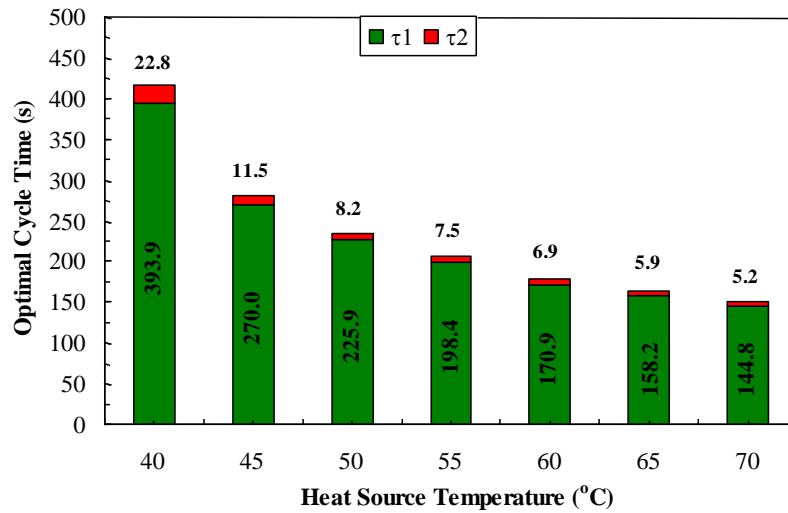**Figure 5.** Optimal cycle time of former six-bed three-stage cycle for different heat source temperature.

Figure 6. Optimal cycle time ratio of former six-bed three-stage cycle for different heat source temperature.
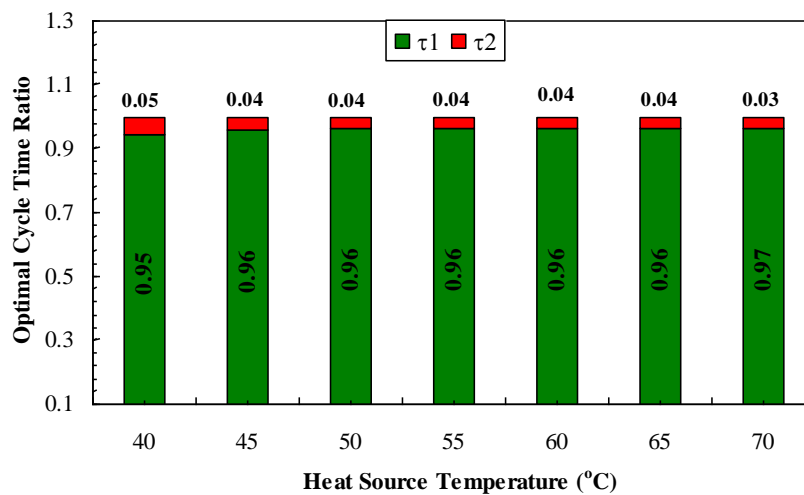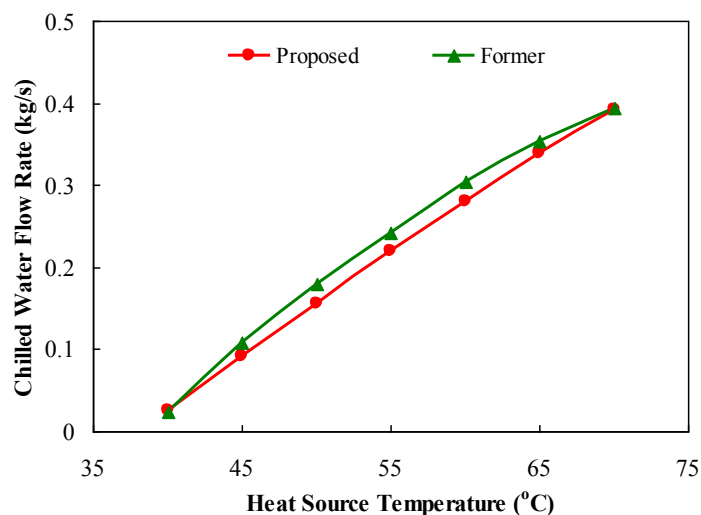

Figure 7. Variation of chilled water flow rate with heat source temperature.

Sensitivity of cycle time on *SCP* of both systems was investigated for a heat source temperature of 60 ℃. *SCP* was calculated by varying the cycle time τ_1 from 20 to 500 s and cycle time τ_2 from 5 to 100 s. The increment steps for τ_1 was 5 s while for τ_2 it was 2.5 s. Chilled water flow rate was kept constant at 0.281 and 0.304 kg s^{-1} for the proposed and former cycle, respectively. These values were observed using the PSO procedure for 60 ℃ heat source temperature. Contour plots of *SCP* of both systems are shown in Figures 8 and 9, respectively. It was clear that by increasing of τ_1, the *SCP* increased to approximately 100 s and after 100 s, it was again decreased (Figure 8). On the other hand, SCP was decreased with the increases of τ_2. A similar profile was also observed in the case of the former system (Figure 9). The contour plot of both systems provided a singular pattern with cycle time. The centre of the contour indicates the maximum *SCP* and corresponding cycle time components, τ_1 and τ_2 indicate the optimal cycle time, which is exactly matching with PSO result.

Figure 8. Contour plot of *SCP* relating to processing time τ_1 and τ_2 at 60 ℃ heat source temperature of proposed system.
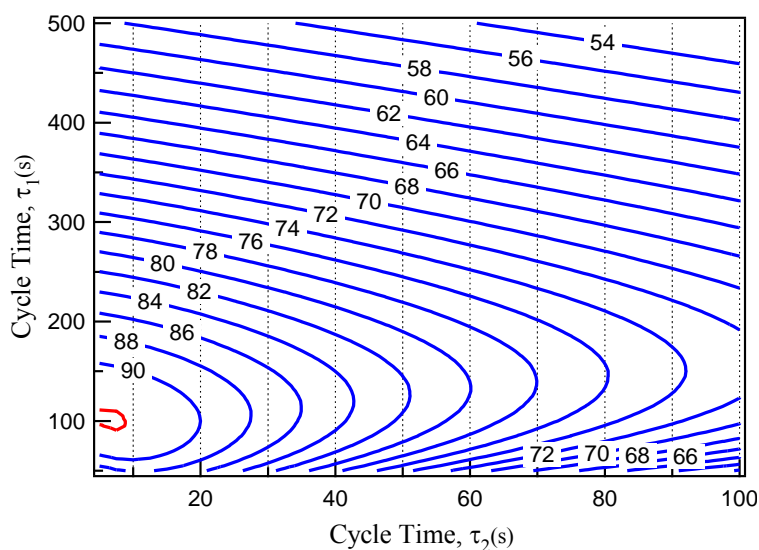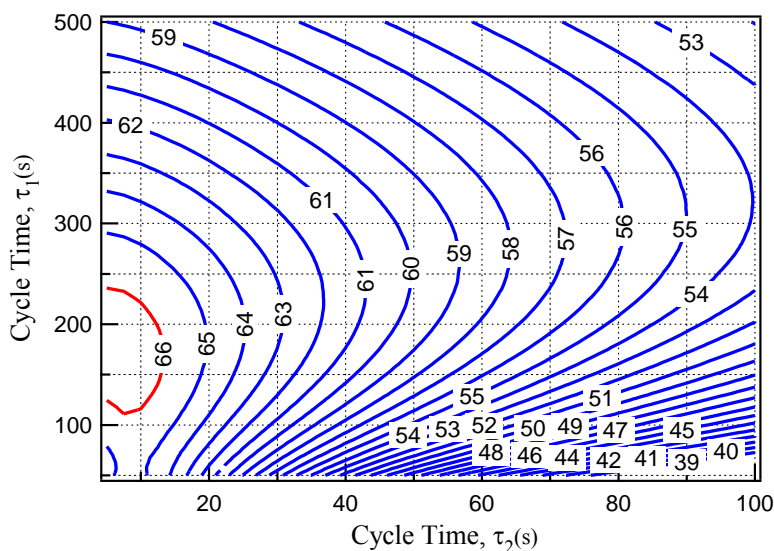

Figure 9. Contour plot of *SCP* relating to processing time τ_1 and τ_2 at 60 ℃ heat source temperature of former system.

The optimal performance of the proposed system is shown in Figure 10. It is apparent that the cycle can operate with a low temperature heat source as low as 40 ℃ and with a coolant at 30 ℃. The *SCP* increased with the increase in heat source temperature, whereas *COP* increased with heat source temperature up to 55 ℃ and then it was decreased slightly with heat source temperature. An increase of heat source temperature with a fixed heat sink causes the system to increase the amount of refrigerant adsorption/desorption promptly, resulting in higher *SCP* at higher heat source temperature. Due to a similar effect, the total optimal cycle time was found to be decreased with heat source temperature, as shown in Figure 11. It is generally observed that the behaviour of *COP* of adsorption cycle increased with longer cycle time. However at lower temperature (<55 ℃), cycle time was found to be increased, whereas *COP* was found to be decreased because at lower driving heat source temperature longer time is needed for effective desorption. The maximum *COP* was observed to be 0.218 at 55 ℃ heat source temperature.

To compare the performance of different adsorption cycles fairly, it is emphasized that the optimized performance of each system should be compared. From this point of view, the optimal performance of the proposed cycle was compared with the optimal performance of the former six-bed three-stage cycle as shown in Figure 10. It can be seen from this figure that both *SCP* and *COP* of the proposed cycle were increased significantly over the whole range of studied heat source temperatures, which is the great benefit of the proposed cycle. Comparison of optimal total cycle time of the proposed cycle with the former six-bed three-stage cycle is also shown in Figure 11. It was observed that proposed cycle provided a little bit longer optimal cycle time at each heat source temperature.

Figure 10. Comparison of optimal *SCP* and *COP* of proposed cycle with the former six-bed three-stage cycle.
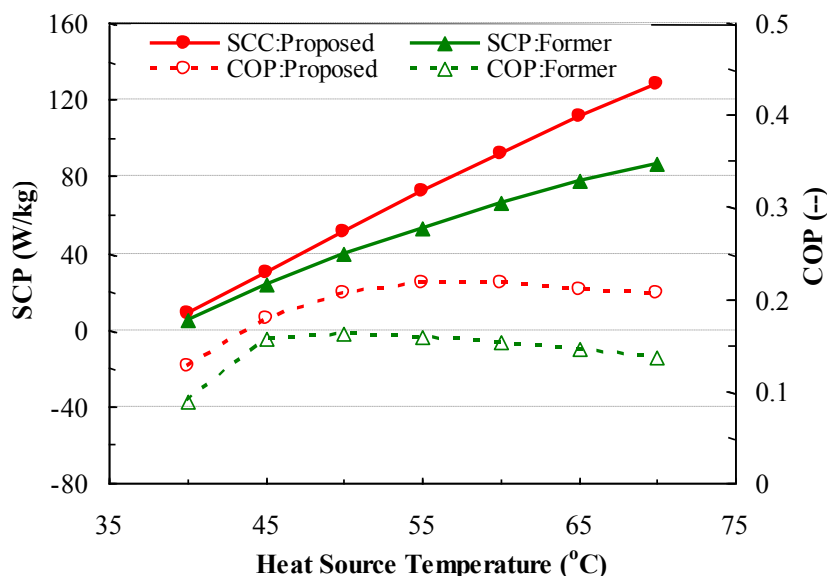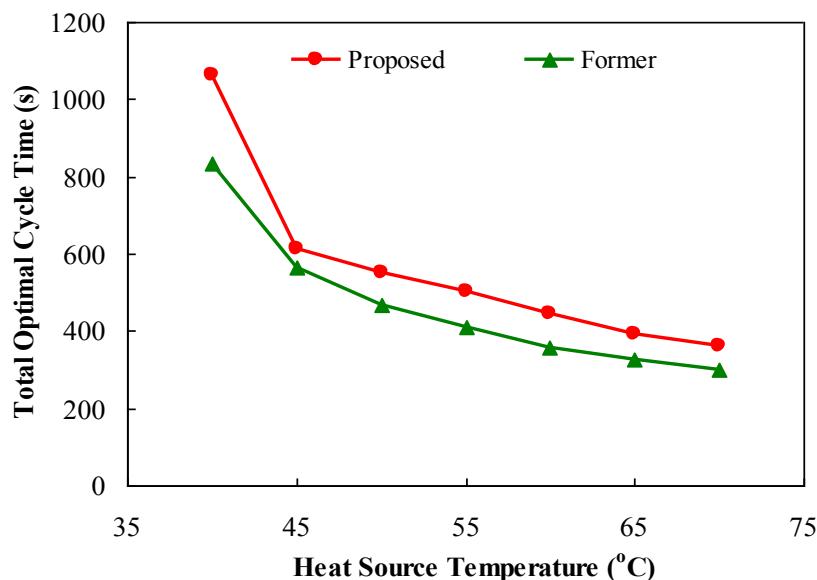
Figure 11. Comparison of optimal cycle time of proposed cycle with the former six-bed three-stage cycle.

The higher *SCP* value of the proposed cycle is due to the effects of the lower total mass of adsorbent (silica-gel) of the system. Because the denominator values as described in Equation (13) is lower as the four beds silica-gel mass is smaller (*i.e.*, 64 kg) than that of six beds of silica-gel (*i.e.*, 96 kg). Heat release as described in the numerator is the same for both systems because both cycles have two beds in lower temper and pressure cycle and producing a similar cooling effect to the evaporator. It is expected mathematically that the *SCP* of four-bed system is larger than that of six-bed system by a factor of 3/2, which was exactly the value achieved in the proposed case.

Although the total cycle time of the proposed system is little bit longer, the proposed cycle provided around 12% to 34% higher *COP* value compare to the former cycle. This is due to a longer adsorption time as well as a shorter desorption time, which is shown in Table 1. Not only that in proposed case, it was observed that adsorption time is more than twice longer than the desorption time as well as the sum of desorption time, pre-cooling and pre-heating time. Aristov *et al.* [31] also gave similar practical recommendations to manage cooling cycles with non-equal durations of adsorption and desorption time. Due to the longer adsorption time the total adsorption of the proposed cycle is higher than that of the the former cycle. As a result *COP* as well as *SCP* were increased over the whole range of heat source temperatures.

A comparative study between the former six-bed three-stage and the proposed four-bed three-stage adsorption system along with improvements due to modification are given in Table 3. Thus, it can be concluded the proposed cycle can significantly reduce the overall size of the three-stage adsorption system while providing an increase in the overall performance.

Table 3. Comparative study of former six-bed three-stage and proposed four-bed three-stage cycle.

Items	Former six-bed, three-stage system	Proposed four-bed, three-stage system
Number of evaporator	1	1
Number of condenser	1	1
Number of beds	6	4
Total mass of Adsorbent	96 kg	64 kg
Total mass of heat exchanger material in beds	12.67 $\times$ 6 kg (Cu) 16.87 $\times$ 6 kg (Al)	12.67 $\times$ 4 kg (Cu) 16.87 $\times$ 4 kg (Al)
Improvements due to the proposed modified design		
Number of bed(s) reduced		2
Reduction in total mass of silica gel		32 kg
Reduction of heat exchanger material		25.34 kg (Cu) 33.74 kg (Al)
COP increased for different heat source temperatures		12% to 34%
SCP increased for different heat source temperatures		21% to 35%

4. Conclusions

A modified design of a four-bed, three-stage adsorption cycle which can be powered by low-temperature thermal energy sources as low as 40 °C has been introduced. A simulation program has been developed to investigate the performance of the system and cycle time was optimized using a particle swarm optimization method. It was observed that the specific cooling power of the proposed innovative cycle increased with heat source temperature. The maximum coefficient of performance of the system was observed for a regeneration temperature at 55 °C. The optimal cycle time was observed to be largely dependent on the corresponding heat source temperature and it decreased with higher heat source temperature when the chilled water outlet temperature was fixed at 9 °C. With the present innovative design, the overall system footprint can be significantly reduced compared to the six-bed three-stage cycle. Moreover, both *SCP* and *COP* were also increased significantly over the whole range of heat source temperatures as compared to that of six-bed three-stage cycle. The proposed cycle could be useful from the economical point of view due to its higher performance and significant reduction in system footprint.

References

1. Saha, B.B.; Kashiwagi, T. Experimental investigation of an advanced adsorption refrigeration cycle. *ASHRAE Trans.* **1997**, *103*, 50–58.
2. Ng, K.C.; Wang, X.L.; Gao, L.; Chakraborty, A.; Saha, B.B.; Koyama, S.; Akisawa, A.; Kashiwagi, T. Apparatus and method for desalination. WO Patent WO/2006/121414 A1, 16 November 2006.
3. Wang, X.; Ng, K.C. Experimental investigation of an adsorption desalination plant using low-temperature waste heat. *Appl. Therm. Eng.* **2005**, *25*, 2780–2789.

4. Wang, X.; Ng, K.C.; Chakarborty, A.; Saha, B.B. How heat and mass recovery strategies impact the performance of adsorption desalination plant: Theory and experiments. *Heat Transf. Eng.* **2007**, *28*, 147–153.

5. Thu, K.; Chakraborty, A.; Saha, B.B.; Chun, W.G.; Ng, K.C. Life-cycle cost analysis of adsorption cycles for desalination. *Desalin. Water Treat.* **2010**, *20*, 1–10.

6. Wu, J.W.; Hu, E.J.; Biggs, M.J. Thermodynamic analysis of an adsorption-based desalination cycle (part II): Effect of evaporator temperature on performance. *Chem. Eng. Res. Des.* **2011**, *89*, 2168–2175.

7. Wu, J.W.; Biggs, M.J.; Pendleton, P.; Badalyan, A.; Hu, E.J. Experimental implementation and validation of thermodynamic cycles of adsorption-based desalination. *Appl. Energy* **2012**, *98*, 190–197.

8. Chua, H.T.; Ng, K.C.; Malek, A.; Kashiwagi, T.; Akisawa, A.; Saha, B.B. Modeling the performance of two-bed, sillica gel-water adsorption chillers. *Int. J. Refrig.* **1999**, *22*, 194–1204.

9. Alam, K.C.A.; Saha, B.B.; Kang, Y.T.; Akisawa, A.; Kashiwagi, T. Heat exchanger design effect on the system performance of silica gel adsorption refrigeration systems. *Int. J. Heat Mass Transf.* **2000**, *43*, 4419–4431.

10. Wang, R.Z. Performance improvement of adsorption cooling by heat and mass recovery operation. *Int. J. Refrig.* **2001**, *24*, 602–611.

11. Uyun, A.S.; Akisawa, A.; Miyazaki, T.; Ueda, Y.; Kashiwagi, T. Numerical analysis of an advanced three-bed mass recovery adsorption refrigeration cycle. *Appl. Therm. Eng.* **2009**, *29*, 2876–2884.

12. Saha, B.B.; Akisawa, A.; Kashiwagi, T. Solar/waste heat driven two-stage adsorption chiller: The prototype. *Renew. Energy* **2001**, *23*, 93–101.

13. Alam, K.C.A.; Saha, B.B.; Akisawa, A.; Kashiwagi, T. Influence of design and operating conditions on the system performance of a two stage adsorption chillier. *Chem. Eng. Commun.* **2004**, *191*, 981–997.

14. Hamamoto, Y.; Alam, K.C.A.; Akisawa, A.; Kashiwagi, T. Performance evaluation of a two-stage adsorption refrigeration cycle with different mass ratio. *Int. J. Refrig.* **2005** *28* 344–352.

15. Khan, M.Z.I.; Saha, B.B.; Miyazaki, T.; Akisawa, A.; Kashiwagi, T. Study on a Two-Stage Adsorption Chiller Using Re-Heat. In *Proceedings of Japan Society of Refrigerating and Air-Conditioning Engineers (JSRAE) Annual Conference-10*, Tokyo, Japan, 2005; pp. 23–27.

16. Khan, M.Z.I.; Alam, K.C.A.; Saha, B.B.; Hamamoto, Y.; Akisawa, A.; Kashiwagi, T. Parametric study of a two-stage adsorption chiller using re-heat-the effect of overall thermal conductance and adsorbent mass on system performance. *Int. J. Therm. Sci.* **2006**, *45*, 511–519.

17. Khan, M.Z.I.; Alam, K.C.A.; Saha, B.B.; Akisawa, A.; Kashiwagi, T. Study on a re-heat two-stage adsorption chiller–The influence of thermal capacitance ratio, overall thermal conductance ratio and adsorbent mass on system performance. *Appl. Therm. Eng.* **2007**, *27*, 1677–1685.

18. Alam, K.C.A.; Khan, M.Z.I.; Uyun, A.S.; Hamamoto, Y.; Akisawa, A.; Kashiwagi, T. Experimental study of a low temperature heat driven re-heat two stage adsorption chiller. *Appl. Therm. Eng.* **2007**, *27*, 1686–1692.

19. Farid, S.K.; Billah, M.M.; Khan, M.Z.I.; Rahman, M.M.; Sharif, U.M. A numerical analysis of cooling water temperature of two-stage adsorption chiller along with different mass ratios. *Int. Commun. Heat Mass Transf.* **2011**, *38*, 1086–1092.

20. Rahman, A.F.M.M.; Ueda, Y.; Akisawa, A.; Miyazaki, T.; Saha, B.B. Innovative design and performance of three-bed two-stage adsorption cycle under optimized cycle time. *J. Environ. Eng.* **2012**, *7*, 92–108.

21. Wang, J.; Wang, L.W.; Luo, W.L.; Wang, R.Z. Experimental study of a two-stage adsorption freezing machine driven by low temperature heat source. *Int. J. Refrig.* **2012**, in press, doi: 10.1016/j.ijrefrig.2012.10.029.

22. Alam, K.C.A. Design Aspects of Adsorption Refrigeration Systems. Ph.D. Thesis, Tokyo University of Agriculture and Technology, Tokyo, Japan, March 2001.

23. Moriyama, K. Performance Improvement of Adsorption Chillers by the Optimization of Cycle time Component. Master's Thesis, Tokyo University of Agriculture Technology, Tokyo, Japan, March 2007.

24. Saha, B.B.; Boelman, E.C.; Kashiwagi, T. Computational analysis of an advanced adsorption-refrigeration cycle. *Energy* **1995**, *20*, 983–994.

25. Khan, M.Z.I.; Alam, K.C.A.; Saha, B.B.; Akisawa, A.; Kashiwagi, T. Performance evaluation of multi-stage, multi-bed adsorption chiller employing re-heat scheme. *Renew. Energy* **2008**, *33*, 88–98.

26. Saha, B.B.; Akisawa, A.; Kashiwagi, T. Silica gel water advanced adsorption refrigeration cycle. *Energy* **1997**, *22*, 437–447.

27. Glueckauf, E. Theory of chromatography. Part 10–Formula for diffusion into spheres and their application to chromatography. *Trans. Faraday Soc.* **1955**, *51*, 1540–1551.

28. Sakoda, A.; Suzuki, M. Fundamental study on solar powered adsorption cooling system. *J. Chem. Eng. Jpn.* **1984**, *17*, 52–57.

29. Akahira, A. Research on the Advanced Adsorption Refrigeration Cycles with Vapour Recovery. Ph.D. Thesis, Tokyo University of Agriculture and Technology, Tokyo, Japan, March 2004.

30. Kennedy, J.; Eberhart, R. Particle Swarm Optimization. In *Proceedings of IEEE International Conference on Neural Networks*, Perth, WA, USA, 27 November–1 December 1995; Volume 4, pp. 1942–1948.

31. Aristov, Y.I.; Sapienza, A.; Ovoshchnikov, D.S.; Freni, A.; Restuccia, G. Reallocation of adsorption and desorption times for optimization of cooling cycles. *Int. J. Refrig.* **2012**, *35*, 525–531.